scientific reports

Check for updates

OPEN

Submarine groundwater discharge and associated fluxes along the Kanyakumari coast of India using radon and nutrient mass balance approach

Annmaria K. George[1], M. Suresh Gandhi[1], P. Muthukumar[2], Priyadarsi D. Roy[3], A. Baalamurugan[2], Muralitharan Jothimani[4]✉ & S. Selvam[2]✉

Submarine groundwater discharge (SGD) acts as a carrier for elements, nutrients and pollutants into the ocean. This study estimated SGD along the Kanyakumari coast of India, using the Radon and nutrient mass balance approach. Groundwater and porewater samples during the high-tide and low-tide conditions showed Radon (^{222}Rn) concentrations between 11.68 and 66.96 Bq/L during the pre-monsoon and between 18.9 and 189.56 Bq/L during the post-monsoon, with an inverse relationship with EC (256–52400 µS/cm: pre-monsoon and 329–48000 µS/cm: post-monsoon). SGD, estimated using the radon mass balance approach, ranged from 0.01 to 0.54 $m^3m^{-2}d^{-1}$ in pre-monsoon and 0.04 to 0.98 $m^3m^{-2}d^{-1}$ in post-monsoon. Mean nutrient concentrations for DIN, DIP, and DSi in both seasons were 0.79-2.0, 0.21–0.28, and 17.22–20.75 µmol L^{-1}, respectively. In a strategic part of Indian coast, this study enabled the location and determination of SGD and thereby provided valuable data for adopting proper methodology to mitigate the issue of groundwater scarcity and pollution.

Keywords Coastal groundwater, Seasonal variation, Radon and nutrient fluxes, Arabian sea

Submarine groundwater discharge (SGD) refers to the natural process of groundwater flow into the ocean through coastal margins. Hence, the understanding and quantifying of SGD is essential, especially for regions with long coastlines, as significant volumes of groundwater that could potentially be harnessed to meet the present-day demand for drinking and irrigation gets lost unnoticed[1]. SGD can also act as a carrier for various pollutants such as heavy metals, micronutrients, and pesticides from the land to the sea[2,3]. Different human activities have contributed to increase the nutrients in coastal waters in recent years[4]. Contaminants from the sewage, agricultural runoff, fertilizers, pesticides and industrial effluents often pollute the coastal aquifers, making the SGD a pathway to reach the ocean. This can lead to harmful algal blooms, red tides, low oxygen zones, and loss of marine biodiversity[5]. Moreover, the interactions between seawater and freshwater within the coastal aquifers significantly impact the coastal ecosystems[6]. The dynamics of groundwater discharge in coastal areas are highly complex, being strongly influenced by the tidal cycles, which can shift the location, volume, composition, and even the direction of SGD multiple times a day[7]. Hence, the accurate assessment and monitoring of SGD are vital for the sustainable management and protection of coastal environments.

Several methodologies have successfully estimated the SGD along coastal zones that include: Seepage meters, Hydrologic models, Remote sensing, Isotope tracing, Water balance approaches, Hydrogeochemistry and Resistivity survey[8–10]. Among all these, the isotope tracing serves as an important technique for identification and quantification of SGD. The radon isotopes have proven to be highly effective for detecting and quantifying SGD[11–13]. Groundwater tends to have significantly higher concentrations of radon (^{222}Rn) compared to surface waters, often by 2 to 4 orders of magnitude. This difference makes it possible to detect even small amounts of radon

[1]Department of Geology, University of Madras Guindy campus, Chennai, India. [2]Department of Geology, V.O. Chidambaram College, Thoothukudi 628008, Tamil Nadu, India. [3]Instituto de Geología, Universidad Nacional Autónoma de México (UNAM), Ciudad Universitaria, 04510 Ciudad de México, Mexico. [4]Department of Geology, College of Natural and Computational Sciences, Arba Minch University, Arba Minch, Ethiopia. ✉email: muralitharan.jothimani@amu.edu.et; geoselvam10@gmail.com

in coastal waters despite the dilution[1,14]. The naturally occurring radionuclide ^{222}Rn, with a half-life of 3.8 days, is widely utilized as a tracer in SGD studies[15,16]. Radon is generated within aquifers through the decay of ^{226}Ra in mineral matrices, while its presence in surface waters is minimal due to a lack of production sources. This stark contrast in concentration levels enables the identification of SGD zones and the estimation of discharge rates using radon measurements[17]. The radon mass balance approach originally developed and subsequently refined by the authors Burnett and Dulaiova and is widely used to quantify submarine groundwater discharge (SGD) fluxes[14,15,18]. The input of nutrient into the ocean via SGD can be estimated by multiplying this flux with average nutrient concentrations in the groundwater[19]. Hence, the understanding of SGD and the associated nutrient transport are vital for protecting and managing the coastal ecosystems[20]. Although the occurrence of SGD along the southwest coast of India at Kanyakumari has been previously reported, the present study offered the first detailed quantitative evaluation of SGD using the combined methods of radon and nutrient mass balance. The relationship between radon concentration, electrical conductivity and nutrient levels helped to demarcate the areas of major discharge and highlights their influence on coastal nutrient dynamics and water quality.

Study area

Kanyakumari district lies in the southernmost part of the Indian subcontinent at the coast of Indian Ocean, between latitude 8˚10' and 8˚15'N and longitude 77˚10' and 77˚20'E (Fig. 1). This area features a diverse landscape of rocky shores and sandy beaches and serves as the meeting point of the Bay of Bengal and the Arabian Sea, making it a distinctive geological formation. The major rivers flowing in the region are Pazhayar, Valliyar, and Tamiraparani[21]. The estuarine ecosystems in areas like Thengapattinam and Manakudi provide crucial habitats for mangroves, mudflats, and diverse avian species, contributing to the region's ecological richness.

Rainfall and climate

Kanyakumari has a tropical coastal climate with moderate to high humidity throughout the year. It receives rain from both the Southwest (June-September) and Northeast monsoons (October-December), making it one of wettest districts of the Tamil Nadu state[22]. The average annual rainfall ranges from 1,000 to 1,400 mm. Summers (March-May) are pleasant, with temperatures ranging from 25 to 35 °C, and winters (December-February) are mild, with temperatures ranging from 20 to 30 °C. The region's coastline influences its climate, ensuring both the constant temperature and frequent sea breeze.

Geology and hydrogeology

Lithology of the area primarily consists of charnockites, khondalite, migmatite, laterites, sandstones, variegated clay, and river alluvium[23,24]. The region's aquifer system is composed of unconsolidated to semi-consolidated formations and fractured crystalline rocks. In hard-rock terrains, the thickness and nature of weathered zone vary both laterally and with depth, significantly influencing the groundwater recharge. Groundwater in alluvial formations exists under water table conditions and generally occurs in an unconfined state.

Materials and methods

^{222}Rn in groundwater and porewater

Fifty-eight water samples (29 groundwater and 29 porewater) were collected during pre-monsoon (May 2023) and post-monsoon (January 2024) seasons based on the tidal fluctuations (Table 1). In-situ parameters like pH, EC (Electrical conductivity), TDS (Total Dissolved Solids), Temperature and Salinity were measured from the field itself using portable water quality analyzer. Samples for radon and nutrients (nitrate, phosphate and silicates) analysis were transported to the laboratories immediately after the sampling. Nutrient analysis was carried out using spectrophotometric methods and Radon analysis was done using RAD7 instrument within 8 h of sampling. Groundwater from inland wells and porewater near the shoreline were collected using 250 ml glass bottles. Porewater was collected from the intertidal zone at a depth of 1.5 m using push point sampler and the groundwater was collected from the wells of the nearby houses.

RAD7 (Durridge Company Inc) is a widely used instrument for measuring ^{222}Rn in water samples and it helps to track freshwater inflows into coastal areas[26]. A sealed water sample (250 ml) was collected and placed in an air-tight bubbling chamber, where radon gas was transferred from water to air. The radon-enriched air was then circulated through the RAD7's electrostatic sensor, which detected radon decay by identifying the charged polonium isotopes. The device displayed radon levels in Bq/m³ (or pCi/L), which then got converted to water concentrations using a partition coefficient. Higher radon levels in coastal waters indicated SGD presence, helping estimate the groundwater flux.

RAD7 calibration and measurement principle

The calibration involved comparison with a secondary standard radon chamber, achieving a reproducibility better than ± 2% and an overall accuracy of ± 5% under standard temperature and humidity conditions. Annual recalibration is recommended by the manufacturer to ensure the accuracy. RAD7 operates on an electrostatic detection principle, and its internal algorithm converts alpha counts to radon activity concentration (Bq m^{-3}) using the calibration factor, and automatically applies corrections for temperature, humidity and background counts.

In Normal mode, the working range is 0.1–400,000 Bq m^{-3}, with a minimum detectable concentration (MDL) of approximately 0.4 Bq m^{-3} (for a 1-hour cycle at 5% relative humidity). In WAT-250 mode, which involves equilibrating dissolved radon between water and a closed air loop using an aeration bottle of 250 mL, the system detects concentrations as low as 0.37 Bq L^{-1} depending on counting time and loop volume. The

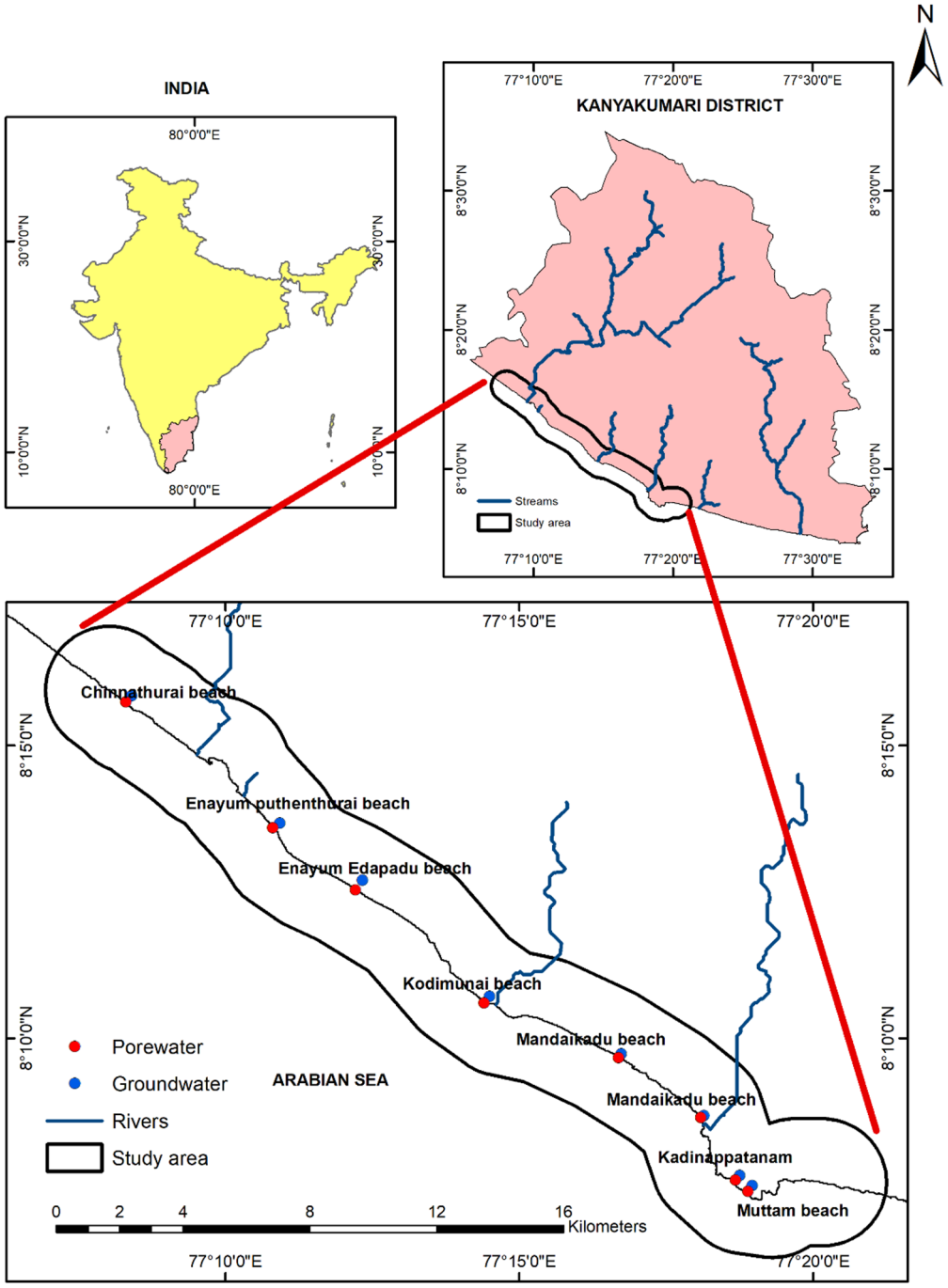

Fig. 1. Location map of Kanyakumari coastal zone in southernmost India and the sampling points of groundwater and porewater for the submarine groundwater discharge estimation.

overall measurement uncertainty combining calibration error and counting statistics was estimated at ± 10% for all reported radon concentrations.

Radon-based mass balance approach

Radon mass balance approach is a scientific tool that measures the movement and concentration of radon (more especially, ^{222}Rn) within a system[4,27,28]. This method basically applies the principle of mass conservation to track the flow of radon through an environment. It is frequently used to estimate groundwater discharge rates in coastal areas by measuring radon levels in both surface and groundwater[29]. SGD estimation protocol for the radon mass balance model was detailed in Table 2 and in Eq. (1) as follows[14]:

$$\mathbf{J_{benthic}} + \lambda \mathbf{I_{Ra}} - \mathbf{J_{atm}} - \lambda \mathbf{I_{Rn}} \pm \mathbf{J_{hor}} = \mathbf{0} \quad (1)$$

	Date	Time	Tide	Height
Pre-monsoon	18 May 2023	00.25 am	High	0.53 m
		6.23 am	Low	0.07 m
		1.13 pm	High	0.79 m
		7 39 pm	Low	0.19 m
	19 May 2023	1.01 am	High	0.53 m
		6.52 am	Low	0.04 m
		1.44 pm	High	0.81 m
		8.08 pm	Low	0.15 m
Post-monsoon	26 January 2024	2.27 am	High	0.74 m
		8.57 am	Low	0.12 m
		2.37 pm	High	0.15 m
		8.11 pm	Low	0.09 m
	27 January 2024	2.53 am	High	0.75 m
		9.16 am	Low	0.1 m
		3.08 pm	High	0.55 m
		8.42 pm	Low	0.09 m

Table 1. Tidal schedule for sample collection at Kanyakumari Coast of southernmost India (Tide-forecast 2024)[25].

Parameter	Description/Symbol	Measurement protocol	Instrument/Source	Units	Uncertainty (±)
Benthic Radon Flux	$J_{benthic}$	Derived from radon concentration gradient (porewater vs. bottom water) using Fick's first law; advective flux from seepage rate × radon concentration	RAD7 (Durridge Co., USA) WAT-250 protocol	Bq m^{-2} d^{-1}	± 10%
Radon Decay Constant	λ	Calculated from half-life of ^{222}Rn (3.823 d) using ($\lambda = \ln(2)/t_{1/2}$)	Physical constant	s^{-1}	Negligible
Radium Inventory (^{226}Ra)	I_{Ra}	Determined from ^{226}Ra decay to ^{222}Rn using RAD7 in WAT-250 mode after 21 days ingrowth under sealed conditions[30]	RAD7 (Durridge Co., USA)	dpm m^{-2}	± 10%
Atmospheric Radon Flux	J_{atm}	Calculated from ($J_{atm} = k\ (C_w — C_{eq})$; *k* derived from wind-speed empirical models.	Meteorological data + empirical model	Bq m^{-2} d^{-1}	± 10%
Radon Inventory	I_{Rn}	Integrated radon concentrations from surface water measured using RAD7 in Normal mode (closed-loop, 30 min cycles).	RAD7 (Durridge Co., USA)	Bq m^{-2}	± 10%
Horizontal Mixing Term	J_{hor}	Estimated from ($K_x \times \Delta C_{Rn}/\Delta_x$); ($K_x$) from tidal amplitude and current velocity[31]	Hydrodynamic model	Bq m^{-2} d^{-1}	± 15%

Table 2. Measurement protocol for radon mass balance model of this study.

where

$\mathbf{J_{benthic}}$ = Total radon input from both advective and diffusive processes in the water column.
$\boldsymbol{\lambda}$ = Decay constant of ^{222}Rn.
$\mathbf{I_{Ra}}$ = Radium inventories.
$\mathbf{I_{Rn}}$ = ^{222}Rn inventories.
$\mathbf{J_{atm}}$ = Atmospheric radon flux.
$\mathbf{J_{hor}}$ = Horizontal mixing of ^{222}Rn.

The balance between radioactive decay, atmospheric loss, and mixing is used to calculate net radon flux[14]. The amount of radon in sediment porewater is estimated since groundwater carries radon from underground sources[11]. The calculated radon flux from SGD can then be converted into a water flux by dividing by the radon concentration in groundwater. It is also assumed that no river runoff affects the study area, ensuring that the primary source of radon is groundwater rather than riverine input. This assumption is supported by field evidence that the Kanyakumari coast lacks perennial river inflow and industrial or sewage discharge points. Sediment porewater and nearshore groundwater exhibited radon concentrations of one to two orders of magnitude higher than the surface seawater, confirming groundwater as the dominant source. The sandy, permeable coastal sediments and gentle hydraulic gradients in this area further facilitate the radon transport through the submarine groundwater discharge.

Additionally, the radon loss is considered to occur mainly due to radioactive decay and atmospheric evasion, neglecting other minor processes that could contribute to its removal. Minor removal mechanisms such as adsorption onto suspended particulates, biological uptake and molecular diffusion across stratified layers were neglected. These processes typically contribute less than 5% to total radon loss in shallow, well-mixed nearshore systems and are therefore considered insignificant relative to atmospheric evasion and radioactive decay. Another key assumption is that the water column is well-mixed, meaning there is no significant stratification in radon distribution. This ensures that the measured radon concentrations are representative of the entire water column rather than being confined to specific layers. These assumptions help streamline the calculation and improve the accuracy of SGD estimates.

Dissolved inorganic nutrients

SGD serves as an important pathway of dissolved inorganic nutrients to the coastal waters[12]. Dissolved Inorganic Nitrogen (DIN), Dissolved Inorganic Phosphorus (DIP), and Dissolved Silicate (DSi) represent the inorganic forms of nitrogen, phosphorus and silica respectively, which are often considered key nutrients that are released from land into the ocean, sometimes contributing significantly to the coastal nutrient levels and impacting the marine ecosystems. The SGD-mediated inflow of nutrients can significantly impact coastal ecosystems and the water quality, altering levels of dissolved and gaseous metabolites, including ammonium, methane, and hydrogen sulfide[13,32]. Multiplying this average nutrient concentration by calculated SGD rates results in the nutrient fluxes[33].

Measurement of DIN, DIP and DSi parameters

All nutrient concentrations were measured using a double-beam UV–VIS spectrophotometer (Model 2203, Systronics). Calibration was performed using certified 1000 mg L^{-1} stock standards with three working standards of 1, 2, and 3 mg L^{-1} prepared for each analyte. The absorbance–concentration relationship showed good linearity (R^2> 0.99). Each sample was analyzed in triplicate, and the mean value was reported. The analytical precision, based on replicate measurements, was within ± 5% for DIN, and DIP, and within ± 7% for DSi.

Nitrite in water reacted with sulphanilamide in an acidic medium, forming a diazo compound. This compound subsequently reacted with N-(1-naphthyl)-ethylene diamine dihydrochloride (NEDA), resulting in the formation of a bright pinkish-red azo dye. The absorbance of both the standard solution and the sample was measured at 540 nm following the same procedure[22]. Nitrate in water was quantitatively reduced to nitrite by passing the sample through a copper-cadmium (Cu-Cd) reduction column. The resulting nitrite reacted with sulphanilamide, forming a diazonium salt, which then combines with NEDA to produce a pink-colored dye, measured by absorbance at 540 nm[34].

Orthophosphate levels were measured using the ascorbic acid method by the reaction with ammonium molybdate to produce molybdophosphoric acid[35]. This compound was then reduced to form a blue-colored complex indicating the amount of phosphate with the depth of the blue color. The absorbance of this color was recorded at a wavelength of 880 nm. Similarly, the silicate estimation involved preparing molybdate reagent, metol-sulfate solution, oxalic acid solution, and 50% sulfuric acid, subsequently mixed with the reducing reagent. Absorbance measured at 810 nm, with a blank solution as a reference, indicated the concentration of dissolved silicate. The procedure is repeated for 20 ml samples to determine silicate concentration.

Results and discussion

Physicochemical characteristics

Water samples in pre-monsoon showed pH of 5.6–7.4, with a mean of 6.5 ± 0.4, whereas the post-monsoon samples had pH between 5.4 and 7.53, with a mean of 6.7 ± 0.3 (Fig. 2). Values close to 7 in both groundwater and porewater for both the seasons indicated nearly neutral conditions. EC of pre-monsoon groundwater (256–3770 µS/cm) and porewater (51.5 to 52.4 mS/cm) and the post-monsoon groundwater (329 to 1701 µS/cm) and porewater (36.2 to 38mS/cm) indicated SGD in all the post-monsoon and most of the pre-monsoon sites where groundwater showed EC < 3000 µS/cm[36]. High EC in groundwater from Chinnathurai could be an indication

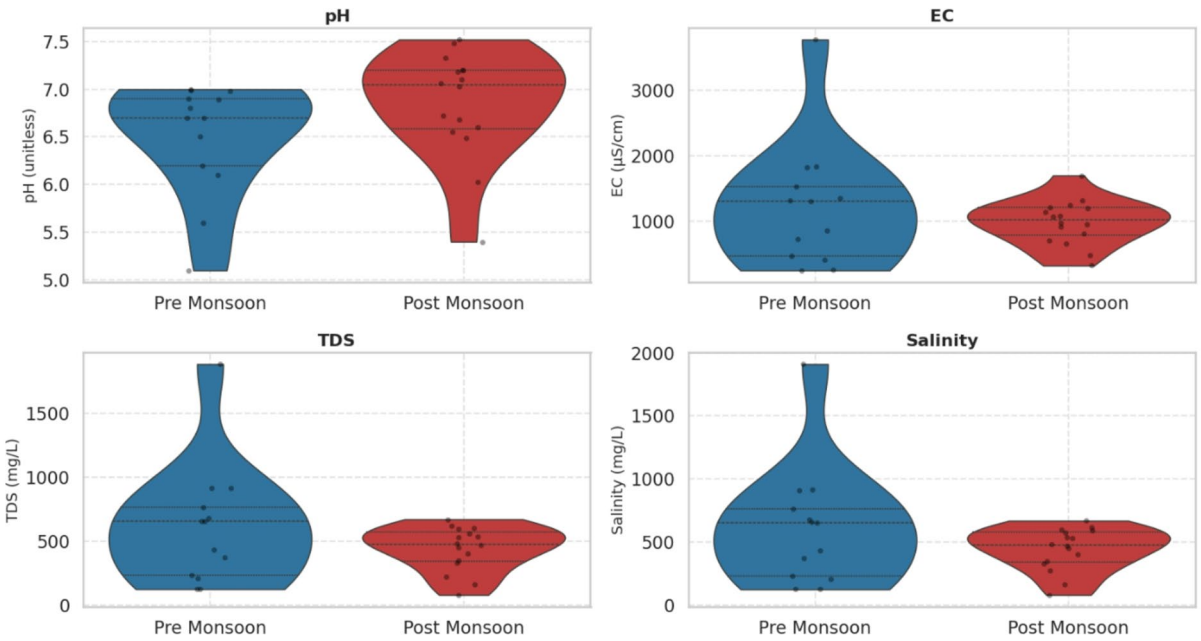

Fig. 2. Variation of physicochemical parameters during pre-monsoon and post-monsoon seasons at Kanyakumari coast of southernmost India.

of seawater intrusion. Enayum Edapadu beach and Mandaikadu beach showed low EC values during both the seasons, which suggested the presence of SGD. EC of porewater remained lower in post-monsoon compared to the pre-monsoon. Highest EC in the pre-monsoon and lowest EC in post-monsoon reflected enhanced evaporation and high salt concentration in the dry pre-monsoon season and dilution of the groundwater from precipitation in the post-monsoon[37]. TDS varied from 128 to 1880 mg/L in groundwater and 25,700 to 28,800 mg/L in porewater during the pre-monsoon. In post-monsoon, It was characterized by 83–672 mg/L in groundwater and 20,500–26,300 mg/L in porewater. The higher salinity of groundwater in the areas with more electrical conductivity indicated seawater intrusion.

Radon concentration in groundwater and porewater

Radon (^{222}Rn) concentration varied between 32.02 and 66.96 Bq/L in groundwater and between 11.68 and 19.77 Bq/L in porewater of pre-monsoon. In post-monsoon samples, the groundwater and porewater had radon of 25.6–189.56 Bq/L and 18.9–41.5 Bq/L, respectively. Some of the groundwater and all the porewater of post-monsoon had more radon. Maximum radon at Muttam Beach during both the seasons possibly reflected radioactive decay of parent ^{226}Ra nuclide from the aquifer matrix[31]. More radon and higher EC indicated saline SGD whereas the higher radon and lower EC demarcated areas of fresh SGD[7]. The spatial distribution of both in sites such as Muttam exhibited elevated levels of radon but comparatively low EC, signifying fresh groundwater discharge into the sea. In contrast, the areas with high EC and low radon values are mainly influenced by seawater intrusion or surface evaporation (Fig. 3). These variations resulted from a combination of environmental and hydrogeological factors. Seasonal fluctuations have modified the groundwater recharge and discharge dynamics, thereby influencing the radon activity and nutrient concentrations[38,39]. Tidal movements have led to intermittent mixing of seawater and groundwater, affecting the salinity and electrical conductivity along the shoreline. The interaction between groundwater and seawater has regulated the transfer of dissolved substances with the fresh groundwater input generally raising both radon[8,40,41] and nutrient levels, and seawater intrusion enhancing EC. Furthermore, the local geological characteristics, including lithology, aquifer structure, and permeability differences, determined the extent and distribution of submarine groundwater discharge along the coastal zone of Kanyakumari.

Dissolved nutrients concentration and distribution

Tables 3 and 4 shows the measured physical parameters, nutrients and radon in groundwater and porewater samples during pre-monsoon and post-monsoon seasons. Nitrate and phosphate in groundwater mainly originate from the natural breakdown of organic matter, the dissolution of minerals, and human-related activities such as the use of fertilizers, application of manure, and discharge of wastewater. Elevated silica levels are likely linked to the weathering of silicate-rich sediments. The patterns of nutrient also differ by location, depending on factors like oxygen availability and biological processes such as nitrification and denitrification within the aquifer. Over-extraction of groundwater, rainfall patterns, and tidal movements also influence the nutrient fluxes[6]. DIN values between 3.04–33.17μmoles/L in groundwater and between 1.22–4.26μmoles/L in porewater of pre-monsoon were higher compared to the post-monsoon (0.37–4.51 μmoles/L; groundwater and 0.13–3.31 μmoles/L; porewater, Fig. 4). Maximum values of DIN in groundwater and pore water were observed at Enayum Edapadu beach and Muttam. DIP of 0.42–5.96 μmoles/L in groundwater in pre-monsoon was higher compared to the post-monsoon (0.23–3.54 μmoles/L). Some pre-monsoon porewater (0.40 to 1.29 μmoles/L), however contained less DIP compared to the post-monsoon (0.13 to 3.31 μmoles/L). High DIP was observed at Chinnathurai and Mandaikadu beach. DSi of groundwater (32.99–314 μmoles/L) and porewater (28.13 to 35.86μmoles/L) in pre-monsoon was more than the post-monsoon (17.47–38.98 μmoles/L; groundwater and 27.04–246.55 μmoles/L; porewater). Maximum values of DSi at Muttam beach in both the seasons showed indication of SGD (Fig. 4). This discharge of DIN, DIP, and DSi into seawater can lead to nutrient buildup, and problems like algal blooms and eutrophication[7,42].

The box plot analysis (Figs. 5 and 6) showed seasonal and tidal differences in nutrient behavior. In pre-monsoon, the concentrations of DSi and DIN were generally higher and more variable, especially at low tide, suggesting active benthic and groundwater contributions when freshwater dilution was minimal. DIP also showed larger fluctuations at low tide, likely due to nutrient release from the surface sediments.

In contrast, the post-monsoon nutrient concentrations were lower and more consistent between tides, indicating that monsoonal runoff and enhanced mixing reduced the relative influence of SGD and sedimentary inputs. Overall, these results demonstrated a clear transition from nutrient enrichment driven by subsurface inputs before the monsoon to a more diluted and well-mixed system after the monsoon season.

Spatial and seasonal variations of radon, nutrients (DIN, DIP, DSi) and salinity

Scatter plots compared the radon (^{222}Rn) concentrations with salinity during the pre-monsoon and post-monsoon periods, and interpreted the SGD patterns. During pre-monsoon, the salinity ranged widely, with one sample (LG1) from Chinnathurai beach showing an exceptionally high salinity (~2000 mg/L). This sample with extremely high salinity and relatively low radon implied mixing with seawater. Higher radon levels with lower salinity suggested stronger SGD from freshwater sources. During post-monsoon, the salinity remained more confined (mostly < 700 mg/L), suggesting increased dilution by the freshwater or precipitation. Many samples exhibited increased radon levels, with some exceeding 100 Bq/L (notably HG8, reaching ~200 Bq/L) (Fig. 7.). Overall higher Radon concentrations in post-monsoon indicated greater SGD due to enhanced groundwater flow. The monsoon cycle significantly impacted SGD dynamics, with post-monsoon conditions favoring more groundwater discharge.

Salinity versus nutrient concentration provided insights about SGD and its role in coastal nutrient dynamics. During pre-monsoon, the high DSi (> 200 μmol/L) at lower salinity levels (< 500 mg/L) suggested

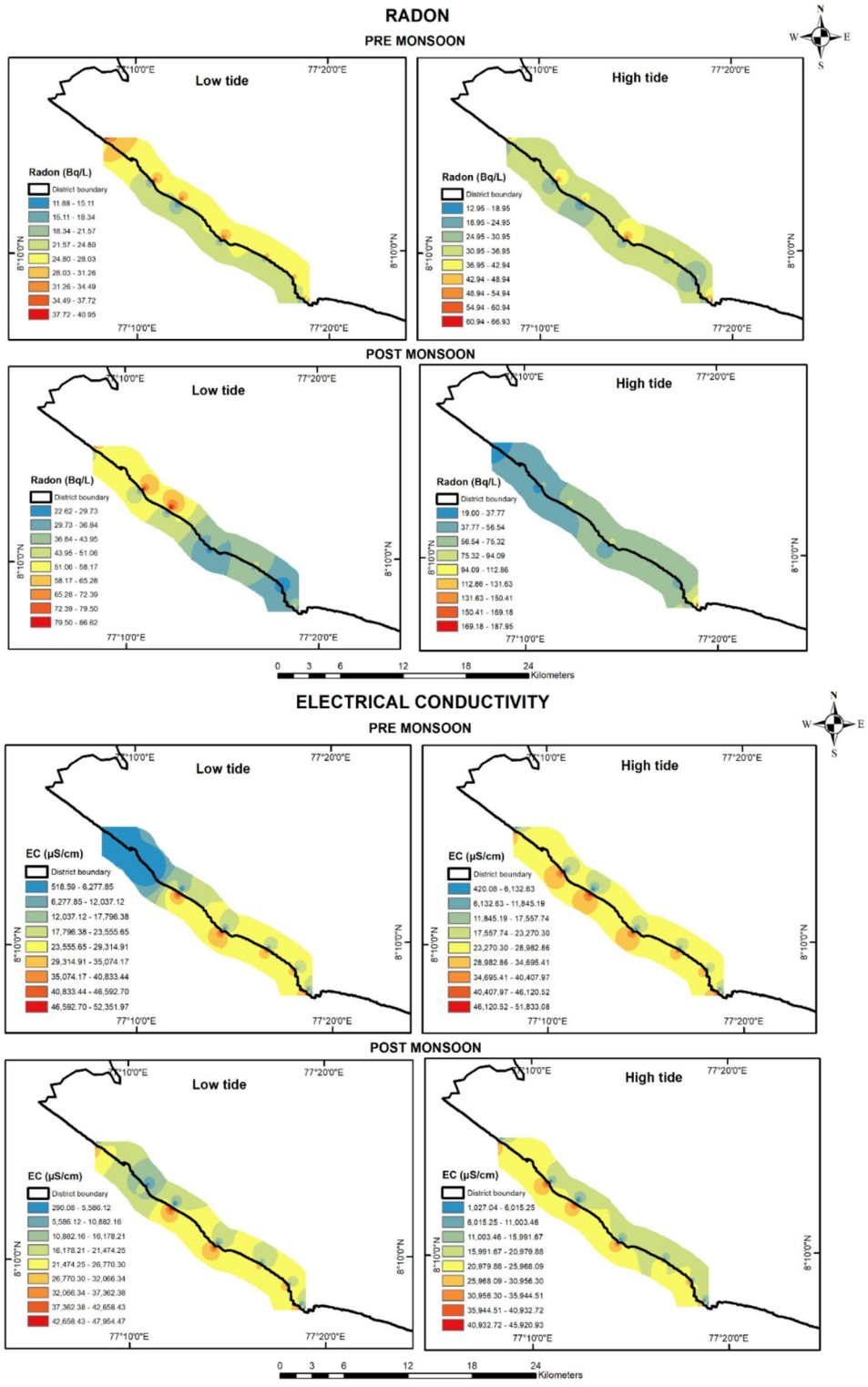

Fig. 3. Radon and EC of the study area during pre-monsoon and post-monsoon seasons at Kanyakumari coast of southernmost India.

a strong terrestrial groundwater influence. Maximum DSi levels with low salinity in samples from Muttam demarcated this location as a probable fresh SGD zone. Higher DIN values at lower salinity levels suggested fresh groundwater as a primary source. During post- monsoon, the DSi concentrations remained significantly lower (< 50 µmol/L), suggesting dilution by rainfall-infiltrated groundwater or changes in groundwater flow paths. DIP concentrations, however, remained consistently low during both the seasons, suggesting limited phosphorus input from SGD (Fig. 8).

Sample name	pH	EC (µS/cm)	TDS (mg/L)	Salinity (ppm)	DSi (µmolL^{-1})	DIP (µmol L^{-1})	DIN (µmol L^{-1})	Radon (Bq/L)
HIGH TIDE								
HG2	6.73	1321	659	654	32.99	0.81	3.04	54.71
HG3	6.21	480	239	235	56.00	0.42	33.17	47.30
HG4	6.91	1829	915	913	211.47	1.11	25.35	58.87
HG5	5.63	261	130	130	243.00	1.64	19.51	48.53
HG6	6.84	736	376	375	224.41	1.81	24.86	38.87
HG7	6.98	1358	679	679	214.11	1.18	4.29	52.24
HG8	6.72	1527	763	763	314.99	2.01	27.20	66.96
HP2	7.30	51,800	28,800	31,700	31.39	0.56	2.08	14.26
HP3	7.42	51,900	25,900	31,800	35.75	0.52	1.58	12.84
HP4	7.33	51,900	25,900	31,700	31.83	0.75	1.56	14.83
HP5	7.12	51,500	25,900	31,700	33.38	1.29	4.26	19.77
HP6	7.14	51,700	25,800	31,700	30.66	0.68	3.19	14.71
HP7	7.36	52,200	26,000	31,900	28.41	0.52	1.96	13.14
HP8	6.91	51,900	25,900	31,800	35.54	0.44	1.85	15.28
LOW TIDE								
LG1	6.99	3770	1880	1910	209.20	5.96	4.00	41.01
LG2	6.89	1307	659	660	225.97	3.12	30.31	37.30
LG3	6.13	422	211	211	195.38	1.74	28.40	36.06
LG4	7.00	1834	916	917	205.10	1.08	28.21	37.3
LG5	5.11	256	128	127	243.56	2.13	14.33	35.84
LG7	6.53	867	433	433	185.17	0.47	27.62	32.02
LP1	7.12	52,400	26,100	32,000	32.58	0.42	1.32	18.98
LP2	7.21	51,600	25,700	31,700	32.09	0.88	3.47	13.48
LP3	7.22	51,600	25,800	31,700	33.04	0.46	1.22	11.68
LP4	7.26	52,400	26,100	32,200	28.13	0.43	1.50	13.82
LP5	7.21	51,800	25,800	31,800	31.13	0.40	1.41	13.59
LP7	7.25	51,700	26,800	31,700	35.86	0.65	1.55	13.59

Table 3. Measured physical parameters, nutrients and radon in groundwater and pore water samples during pre- monsoon season at Kanyakumari Coast of southernmost India.

Radon based estimation of SGD fluxes

Seasonal variation in SGD flux provided insights into groundwater-seawater interactions and the impact of monsoonal recharge on SGD dynamics[6]. SGD flux during pre-monsoon and post-monsoon varied between 0.01 and 0.54 $m^3m^{-2}d^{-1}$ and 0.04 to 0.98 $m^3m^{-2}d^{-1}$, respectively (Fig. 9). Enayum Edapadu beach and Mandaikadu beach showed the maximum flux rate in both the seasons, indicating localized high groundwater discharge zones. Rainfall infiltration recharged the aquifer and increased hydraulic gradients, leading to higher post-monsoon SGD flux[43].

Table 2 lists all radon mass-balance components with propagated 1σ uncertainties for each sample (HG = High Tide Groundwater, HP = High Tide Porewater, LG = Low Tide Groundwater, LP = Low Tide Porewater). Inventory depth (H) was taken as 5 m with ±20% uncertainty. The decay constant of ^{222}Rn (λ) was 0.181 d^{-1} with negligible uncertainty. Atmospheric evasion was computed using a gas transfer velocity (k) of 0.5 ± 10%. Horizontal eddy diffusivity (K_x) was assumed to be 10 ± 15%, with a mixing length of 5–8 m based on nearshore hydrodynamics along the Kanyakumari coast. Diffusive benthic flux (J_{diff}) was approximated as 750 ± 10% Bq m^{-2} d^{-1}. Radon measurement uncertainty (RAD7 calibration and counting statistics) was ± 10%, and SGD flux uncertainty ± 10%. Radium-supported inventory (I_{Ra}) was estimated as 10% of I_{Rn} with ± 10% uncertainty. All uncertainties were propagated using standard variance and multiplicative error propagation rules. The residual term represented the imbalance between total inputs and losses, reflecting unquantified flux components or model simplifications.

Dissolved nutrients mass balance

SGD flux multiplied by the nutrient concentration provided the nutrient mass flux. DSi, DIP and DIN fluxes were higher along Mandaikadu beach in both seasons[44]. During pre-monsoon, the SGD associated dissolved nutrients were 2, 0.21, and 20.75 µmol L^{-1} for DIN, DIP, and DSi, respectively. They were 0.79, 0.28 and 17.22 µmol L^{-1}, respectively, for post-monsoon seasons. More DIN in pre-monsoon period may increase algal blooms in coastal waters. DSi flux was found to be more in both seasons. High DSi suggested prolonged contact with silicate-rich minerals (e.g., quartz, feldspars) during the subsurface flow[42].

Sample name	pH	EC (µS/cm)	TDS (mg/L)	Salinity (ppm)	DSi (µmolL^{-1})	DIP (µmolL^{-1})	DIN (µmolL^{-1})	Radon (Bq/L)
HIGH TIDE								
HG1	7.22	954	472	471	33.42	0.54	0.54	33.50
HG2	7.18	1147	562	573	34.09	0.36	0.37	69.50
HG3	6.55	1220	601	600	32.80	0.68	0.69	88.91
HG4	7.03	814	404	402	29.34	0.66	0.66	95.63
HG5	6.03	1701	83	83	33.43	0.54	0.55	88.45
HG6	7.06	1206	595	595	30.11	3.54	3.54	69.50
HG7	6.68	665	332	331	25.04	1.89	1.89	116.82
HG8	7.48	1075	533	532	33.92	0.79	0.79	189.56
HP1	7.47	46,000	20,500	23,500	27.77	0.28	0.29	36.54
HP2	7.52	45,000	20,500	22,900	28.46	0.33	0.34	18.90
HP3	7.32	42,000	23,000	23,500	36.76	0.57	0.57	29.85
HP4	7.20	43,000	22,000	24,600	32.87	0.77	0.77	27.51
HP5	7.25	36,200	20,500	25,700	62.51	0.13	0.13	42.64
HP6	7.21	44,000	21,500	24,000	224.30	1.06	1.06	36.50
HP7	7.45	42,000	21,000	23,500	246.55	1.24	1.24	28.63
HP8	7.41	37,500	20,500	21,700	202.09	1.71	1.72	33.60
LOW TIDE								
LG1	7.33	920	455	454	32.72	0.49	2.79	74.56
LG2	7.20	976	486	483	33.26	0.23	2.32	84.60
LG3	6.72	329	166	165	38.98	0.77	1.55	86.98
LG4	7.11	480	225	274	17.47	0.78	0.88	44.51
LG5	5.47	1246	620	616	29.06	1.13	4.51	52.33
LG6	6.68	1089	540	539	30.09	0.55	1.36	25.64
LG7	6.49	705	350	350	31.51	0.41	1.67	49.60
LG8	7.52	1326	672	670	37.88	0.35	1.08	29.67
LP1	7.41	48,000	24,000	23,300	31.17	0.65	1.09	33.56
LP2	7.53	43,500	26,300	22,500	32.88	1.10	3.31	26.91
LP3	7.50	48,000	24,000	24,000	31.16	0.59	2.86	25.22
LP4	7.38	48,000	24,000	24,500	29.06	0.36	1.70	22.63
LP5	7.45	42,000	21,500	22,400	33.41	0.33	1.59	29.65
LP6	7.51	47,000	24,000	23,500	32.98	0.35	1.08	29.87
LP7	7.33	48,000	22,000	24,600	27.04	0.79	3.07	24.51
LP8	7.41	41,000	23,000	22,900	33.41	0.43	1.00	41.50

Table 4. Measured physical parameters, nutrients and radon in groundwater and pore water samples during post-monsoon season at Kanyakumari Coast of southernmost India.

Conclusions

Radon is a reliable tracer of SGD in saline environments with distinct enrichment in groundwater relative to the seawater. Here, we used both radon and dissolved nutrients as tracers for quantifying the SGD flux into the Arabian Sea along the western coastal stretch of Kanyakumari at southernmost India. Freshwater SGD was confined along the northern portion of the study area i.e. the Enayam beach. This spatial variation was controlled primarily by differences in coastal geomorphology, permeability and tidal forcing along the shoreline. The radon mass balance quantified SGD flux of 0.01–0.54 $m^3m^{-2}d^{-1}$ during the pre-monsoon and 0.03–1.02 $m^3m^{-2}d^{-1}$ in the post-monsoon. This seasonal variation indicated influence of monsoonal recharge and tidal pumping, which enhanced the groundwater discharge during the post-monsoon. However, the pre-monsoon conditions favored higher nutrient accumulation reflected in the DIN, DIP, and DSi contents of 2, 0.21, and 20.75 µmol L^{-1}, respectively. The post-monsoon conditions promoted dilution and hence reduced the dissolved nitrogen (0.79 µmol L^{-1}) and silicate (17.22 µmol L^{-1}) contents. Insight into these dynamics was important for effective control of coastal nutrient inputs and understanding SGD-driven nutrient fluxes for the sustainable coastal management, especially in a region where anthropogenic and natural processes jointly affect the nutrient dynamics.

Despite the robustness of the radon mass balance approach, certain limitations should be known. The method assumes quasi–steady-state conditions and well-mixed nearshore waters, which may not fully capture short-term variability driven by tidal pumping, wave action, or intermittent recharge events. Uncertainties associated with atmospheric evasion and horizontal mixing terms derived from empirical parameterizations can influence SGD estimates. In addition, the conversion of radon flux to water flux depends on representative groundwater end-member concentrations, which may vary spatially due to aquifer heterogeneity. Furthermore, while radon effectively constrains total SGD, it does not explicitly distinguish between fresh groundwater discharge and

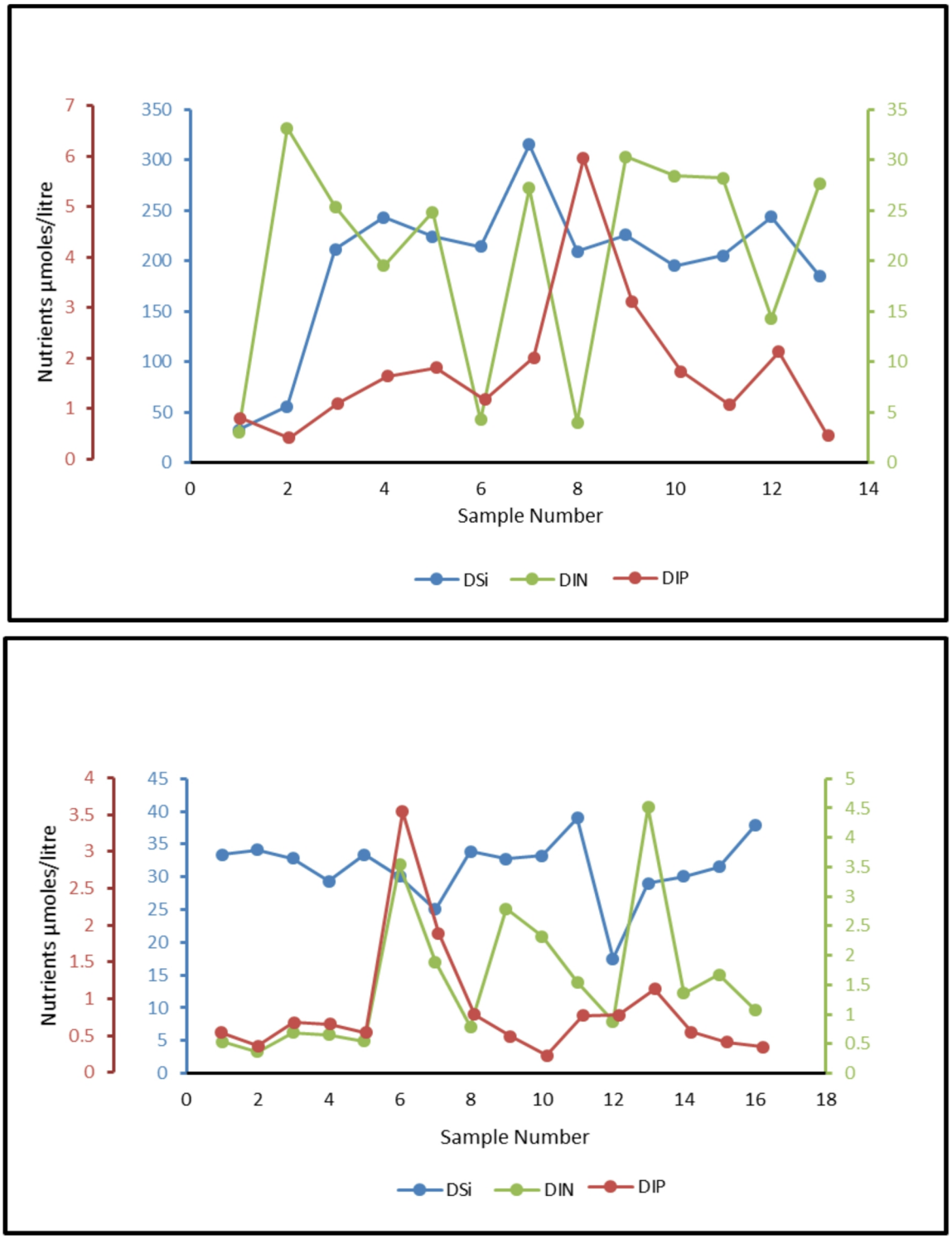

Fig. 4. Spatial distribution of DSi, DIN and DIP during pre-monsoon and post-monsoon seasons at Kanyakumari coast of southernmost India.

recirculated seawater without balancing tracers. Nevertheless, when applied with appropriate hydrological context and uncertainty assessment, the approach remains a powerful tool for quantifying SGD and associated nutrient fluxes in monsoon-influenced coastal systems.

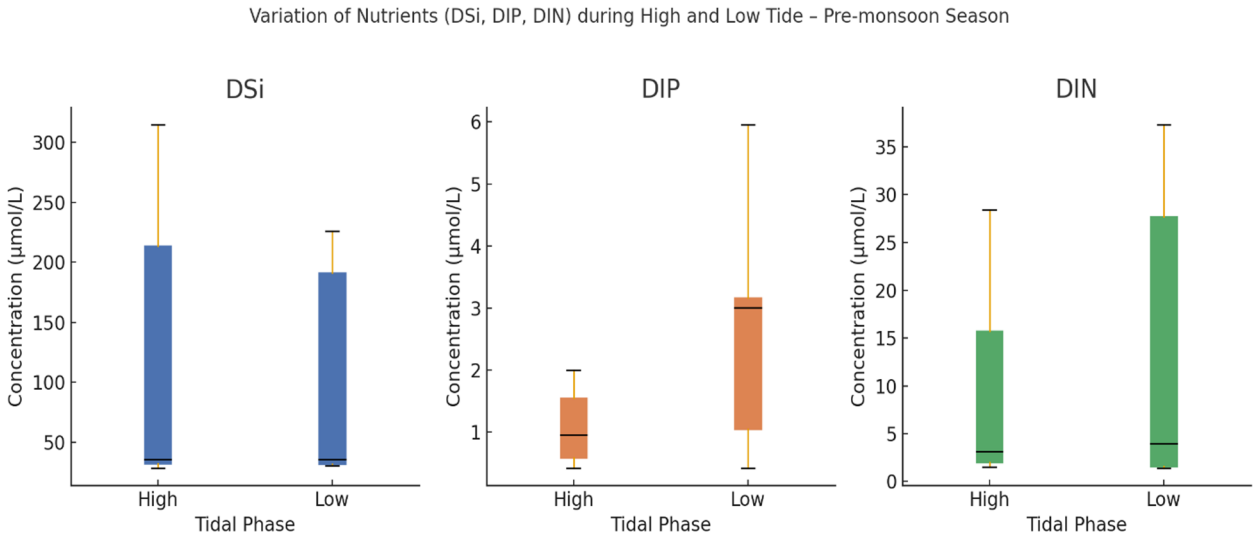

Fig. 5. Variation of nutrients (DSi, DIP and DIN) during pre-monsoon season at Kanyakumari coast of southernmost India.

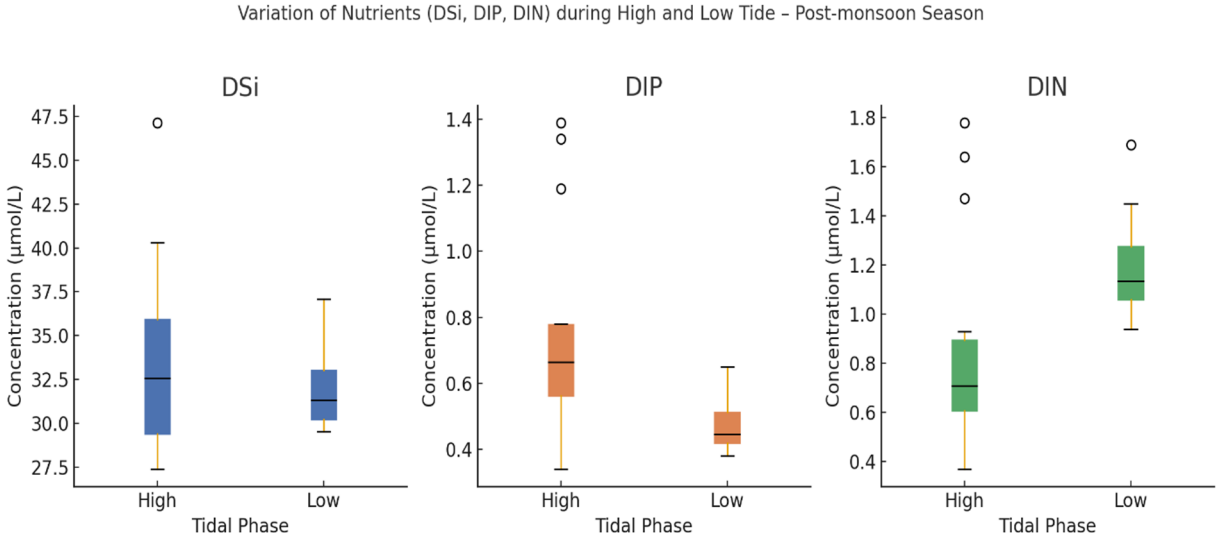

Fig. 6. Variation of nutrients (DSi, DIP and DIN) during post-monsoon season at Kanyakumari coast of southernmost India.

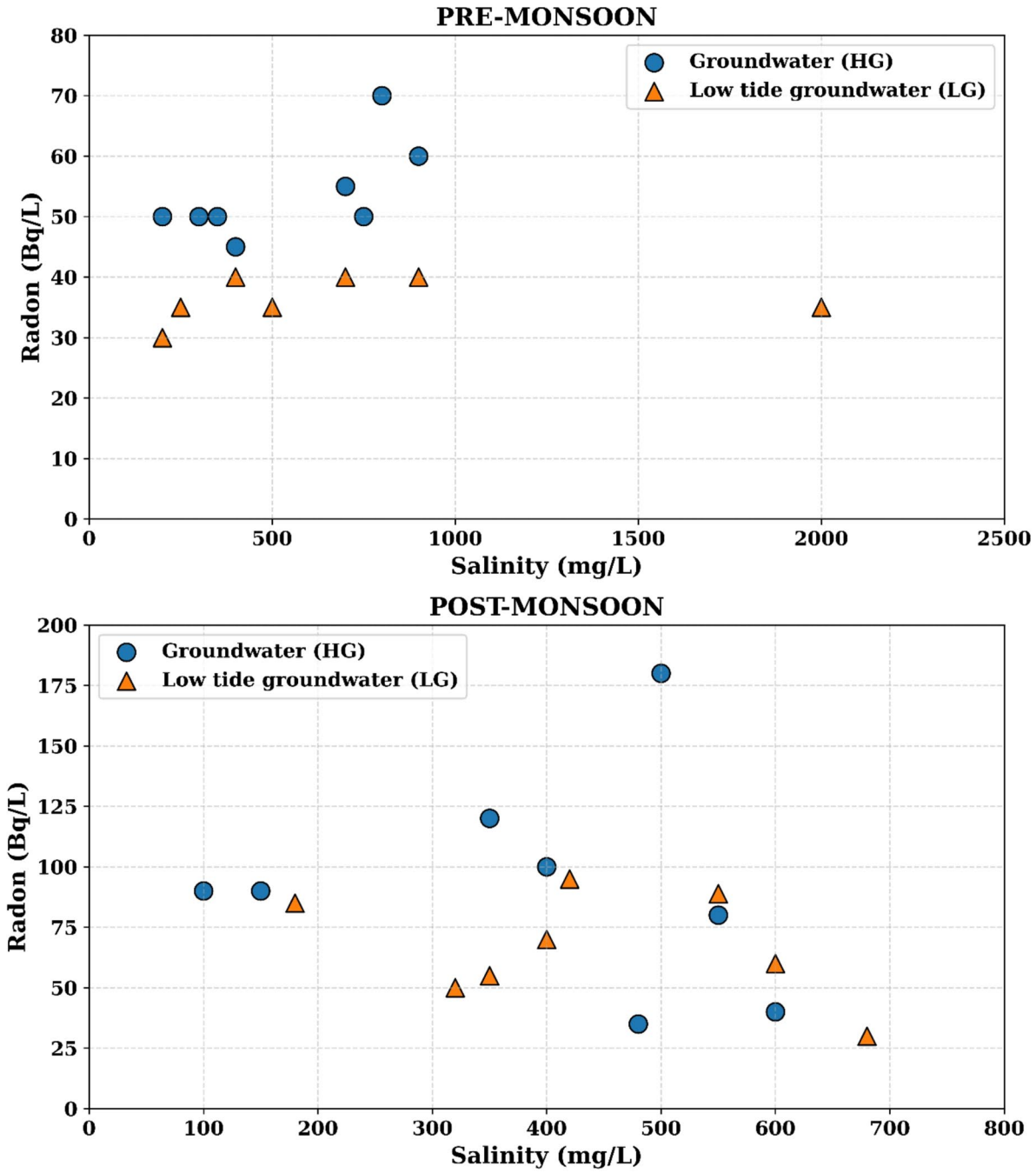

Fig. 7. Radon versus salinity plot for groundwater samples collected during pre-monsoon and post-monsoon seasons at Kanyakumari coast of southernmost India.

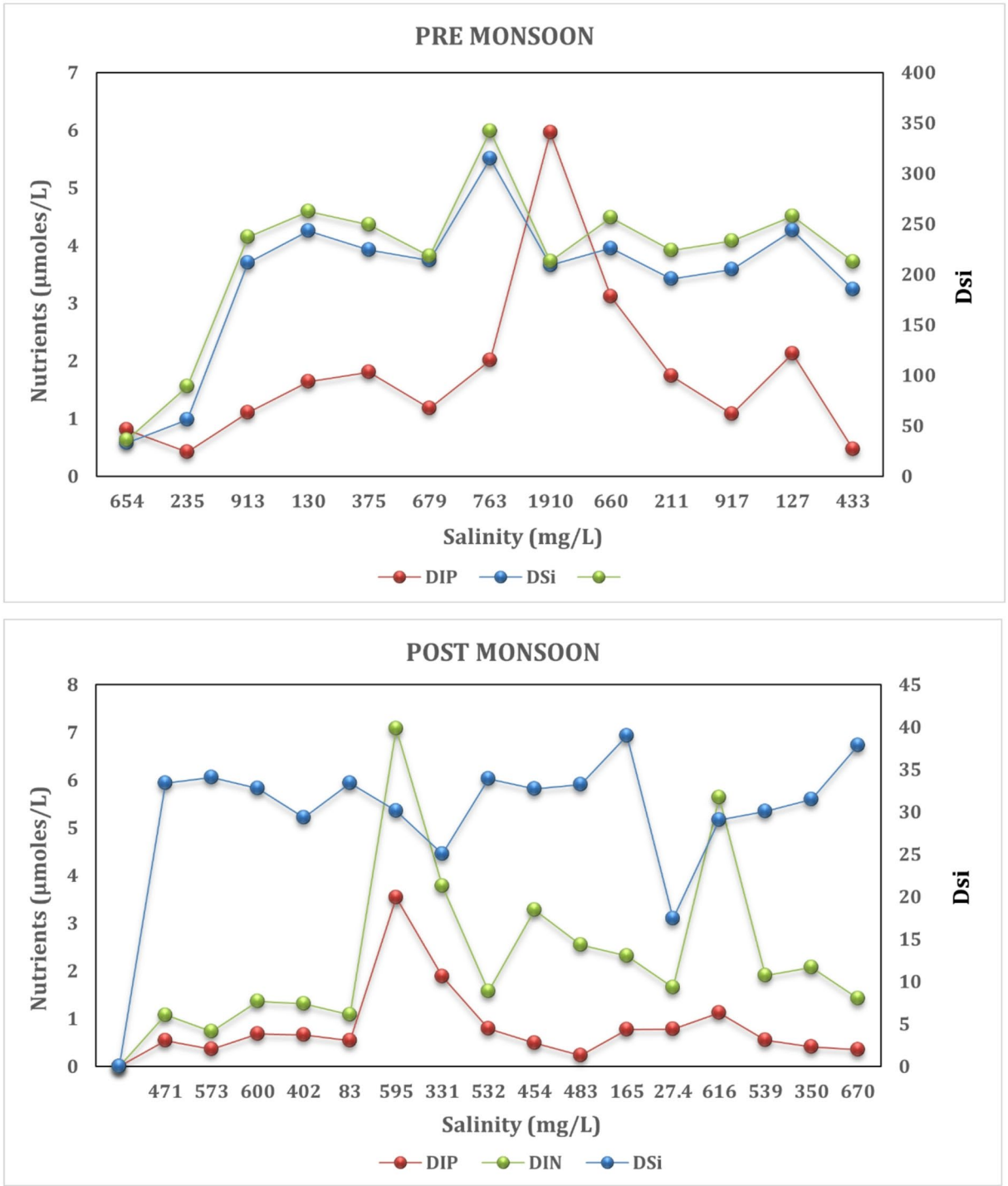

Fig. 8. DIN, DIP, and DSi versus salinity for groundwater samples collected during pre-monsoon and post-monsoon seasons at Kanyakumari coast of southernmost India.

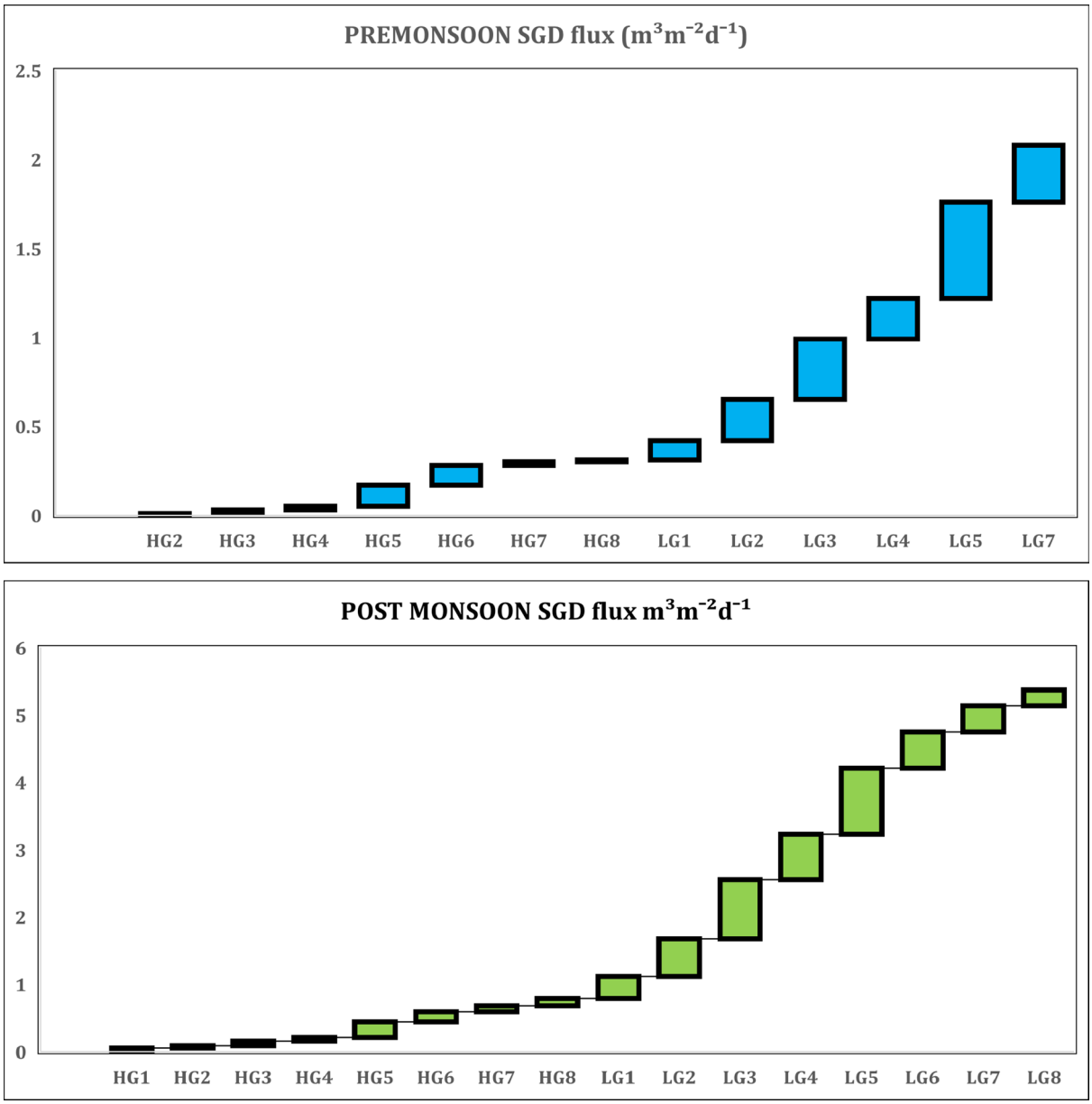

Fig. 9. Observed SGD flux in groundwater during pre-monsoon and post-monsoon seasons at Kanyakumari coast of southernmost India.

Data availability

All data are included in the manuscript.

Received: 10 August 2025; Accepted: 28 January 2026
Published online: 11 March 2026

References

1. Jacob, N., Babu, D. S. & Shivanna, K. Radon as an indicator of submarine groundwater discharge in coastal regions. *Curr. Sci.*, 1313–1320. (2009).
2. Rahman, M. D. et al. Significance of submarine groundwater discharge in the coastal fluxes of mercury in Hampyeong Bay. *Yellow Sea Chemosphere*. **91.3**, 320–327 (2013).
3. Trezzi, G. et al. Submarine groundwater discharge: A significant source of dissolved trace metals to the North Western mediterranean sea. *Mar. Chem.* **186**, 90–100 (2016).
4. Selvam, S. et al. Quantification of submarine groundwater discharge (SGD) using radon, radium tracers and nutrient inputs in Punnakayal, South Coast of India. *Geosci. Front.* **12** (1), 29–38 (2021).
5. Hwang, D. W., Lee, Y. W. & Kim, G. Large submarine groundwater discharge and benthic eutrophication in Bangdu Bay on volcanic Jeju Island. *Korea Limnol. Oceanogr.* **50** (5), 1393–1403 (2005).

6. Gopinath, S., Srinivasamoorthy, K., Prakash, R., Kanna, A. R. & Gopalakrishnan, V. An investigation of submarine groundwater discharge and related fluxes in parts of the Southeast Coast of india: combined radon and nutrients mass balance approach. *Total Environ. Res. Themes*. **6**, 100050 (2023).
7. Krishan, G., Rao, M. S., Kumar, C. P., Kumar, S. & Rao, M. R. A. A study on identification of submarine groundwater discharge in Northern East Coast of India. *Aquat. Procedia*. **4**, 3–10 (2015).
8. Luo, M., Zhang, Y., Li, H., Wang, X. & Xiao, K. Submarine groundwater discharge in a coastal bay: evidence from radon investigations. *Water* **12** (9), 2552 (2020).
9. Douglas, A. R. & Murgulet, D. Groundwater-Surface water interactions in the coastal zone. In *Freshwater Inflows To Texas Bays and Estuaries: A Regional-Scale review, synthesis, and Recommendations* 143–172. (Springer, Switzerland, 2025).
10. Sunilkumar, P. S., Ramesh, H. & Wadde, S. *Advances of Submarine Groundwater Discharge in the Coastal* (A Review, 2025).
11. Taniguchi, M. et al. Spatial and Temporal distributions of submarine groundwater discharge rates obtained from various types of seepage meters at a site in the Northeastern Gulf of Mexico. *Biogeochemistry* **66**, 35–53 (2003).
12. Wang, X., Li, H., Zheng, C., Yang, J., Zhang, Y., Zhang, M., Zhang, X. Submarine groundwater discharge as an important nutrient source influencing nutrient structure in coastal water of Daya Bay, China. Geochimica et Cosmochimica Acta, **225**, 52–65 (2018)
13. Bernard, R. J. et al. Benthic nutrient fluxes and limited denitrification in a sub-tropical groundwater-influenced coastal lagoon. *Mar. Ecol. Prog. Ser.* **504**, 13–26 (2014).
14. Burnett, W. C. & Dulaiova, H. Estimating the dynamics of groundwater input into the coastal zone via continuous radon-222 measurements. *J. Environ. Radioact.* **69**, 21–35 (2003).
15. Burnett, W. C. & Henrieta Dulaiova. Radon as a tracer of submarine groundwater discharge into a boat basin in Donnalucata. *Sicily Cont. Shelf Res.* **26** (7), 862–873 (2006).
16. Petermann, E. et al. Coupling end-member mixing analysis and isotope mass balancing (222-Rn) for differentiation of fresh and recirculated submarine groundwater discharge into Knysna Estuary, South Africa. *J. Geophys. Research: Oceans*. **123** (2), 952–970 (2018).
17. Schubert, M. et al. Radon (222Rn) as tracer for submarine groundwater discharge investigation—limitations of the approach at shallow wind-exposed coastal settings. *Environ. Monit. Assess.* **194** (11), 798 (2022).
18. Dulaiova, H., Camilli, R., Henderson, P. B. & Charette, M. A. Coupled radon, methane and nitrate sensors for large-scale assessment of groundwater discharge and non-point source pollution to coastal waters. *J. Environ. Radioact.* **101** (7), 553–563 (2010).
19. Rodellas, V., Garcia-Orellana, J., Masqué, P., Feldman, M. & Weinstein, Y. Submarine groundwater discharge as a major source of nutrients to the mediterranean sea. *Proc. Natl. Acad. Sci.* **112** (13), 3926–3930 (2015).
20. George, M. E., Akhil, T., Remya, R., Rafeeque, M. K. & Babu, D. S. Submarine groundwater discharge and associated nutrient flux from Southwest Coast of India. *Mar. Pollut. Bull.* **162**, 111767 (2021).
21. Kaliraj, S., Chandrasekar, N. & Ramachandran, K. K. Mapping of Coastal landforms and volumetric change analysis in the South West Coast of Kanyakumari, South India using remote sensing and GIS techniques. *Egypt. J. Remote Sens. Space Sci.* **20** (2), 265–282 (2017).
22. American Public Health Association. Standard methods for the examination of water and wastewater (Vol. 6). American public health association. (1926).
23. George, A. K., Gandhi, M. S., Muthukumar, P. & Selvam, S. Geospatial and analytical hierarchical techniques to assess the groundwater potential areas in Kanyakumari district, Tamil Nadu, India. In Emerging Technologies for Water Supply, Conservation and Management 235–252. (Springer, International Publishing, 2023).
24. CGWB. *Groundwater Year Book—Tamil Nadu and Puducherry, 2019–20* (Central Ground Water Board, Ministry of Jal Shakti, Government of India, 2020).
25. Tide-forecast. January (2024). http://comhttpsd://www.tideforecast.com/locations/Kanniyakumari/tides/latest last accessed on 27.
26. Adyasari, D. et al. Radon-222 as a groundwater discharge tracer to surface waters. *Earth Sci. Rev.* **238**, 104321 (2023).
27. Muthukumar, P. et al. Measurement of submarine groundwater discharge (SGD) into Tiruchendur Coast at Southeast India using 222Rn as a naturally occurring tracer. *Mar. Pollut. Bull.* **174**, 113233 (2022).
28. Sekar, S. & Perumal, M. *Unveiling Hidden Flows: Tracing Submarine Groundwater Discharge in Punnakayal Estuary Coastal region, Tamil Nadu, India, Through Radon (222Rn) and GIS Topology* p.107301 (Marine Environmental Research, 2025).
29. Selvam, S. et al. Submarine groundwater discharge and associated nutrient influx in surroundings of the estuary region at Gulf of Mannar Coast. *Indian Ocean. Chemosphere*. **305**, 135271 (2022).
30. DURRIDGE Company, Inc. (2023). RAD7 Radon Detector User Manual.
31. Burnett, B., Chanton, J., Christoff, J., Kontar, E., Krupa, S., Lambert, M., Taniguchi, M. Assessing methodologies for measuring groundwater discharge to the ocean. Eos, Trans. Am. Geophys. Union, **83** (11), 117–123 (2002)
32. Santos, I. R., Chen, X., Lecher, A. L., Sawyer, A. H., Moosdorf, N., Rodellas, V., Li, L. Submarine groundwater discharge impacts on coastal nutrient biogeochemistry. Nat. Rev. Earth & Environ., **2** (5), 307–323 (2021).
33. Swarzenski, P. W., Reich, C., Kroeger, K. D. & Baskaran, M. Ra and Rn isotopes as natural tracers of submarine groundwater discharge in Tampa Bay. *Fla. Mar. Chem.* **104** (1–2), 69–84 (2007).
34. Strickland, J. D. Hipwell, and Timothy Richard Parsons. A practical handbook of seawater analysis. (1972).
35. Uru, S. K. A critical perspective on the applied potential in amperometric phosphate biosensors. *J. Water Process. Eng.* **58**, 104886 (2024).
36. Manivannan, V., Elango, L. & Narasimhan, C. L. Identification of seawater intrusion and submarine groundwater discharge zones: A case study along the coastal part of South Chennai. *Int. Assoc. Hydrogeol.* **7**, 33–38 (2020).
37. Yadav, A. K. & Khan, P. A comparative study of pre– monsoon and post– monsoon status of different physical and chemical parameters of water samples collected from the various sources of water in Todaraisingh tehsil of Tonk (Rajasthan) India. *Global J.* **13**, 23–32 (2013).
38. Lin, X. et al. Seasonal dynamics of submarine groundwater discharge in Zhanjiang Bay: an investigative study utilizing 222Rn as a tracer. Front. Marine Sci. **11**, 1451533. (2024).
39. George, A. K. et al. Possible zones of submarine groundwater discharge (SGD) and seawater intrusion (SWI) along the West Coast of Kanyakumari, India. *J. Chem.* **2023** (1), 6687308 (2023).
40. Diphofe, K., Diamond, R. & Kotze, F. Quantifying baseflow with Radon, H and O isotopes and field parameters in the urbanized catchment of the little Jukskei River, Johannesburg. *Hydrology* **12** (8), 203 (2025).
41. Schubert, M. et al. Investigating groundwater discharge into a major river under low flow conditions based on a radon mass balance supported by tritium data. *Water* **12** (10), 2838 (2020).
42. Khan, A., Umar, R. & Khan, H. H. Significance of silica in identifying the processes affecting groundwater chemistry in parts of Kali watershed, central Ganga Plain, India. *Appl. Water Sci.* **5**, 65–72 (2015).
43. Kamaraj, J. et al. Radon (222Rn) as a geochemical tracer for submarine groundwater discharge (SGD): measuring techniques, source to sink mass balance model and practical constraints. *Mar. Environ. Res.*, 107639. (2025).
44. George, A. K., Gandhi, M. S. & Joseph, A. M. Groundwater quality assessment of Western coastal zone of Kanyakumari District, Tamil Nadu, India, using Statistical, water quality index and GIS techniques. In *Groundwater Resource Management Planning Strategies: A Geospatial Approach,* Vol. 1 775–793. (Springer, Switzerland, 2025).

Acknowledgements
This study forms part of the Ph.D. research of the first author at the University of Madras. The first author acknowledges the Department of Science and Technology (DST–INSPIRE Fellowship No. DST/INSPIRE Fellowship/IF190592), Government of India, for financial support toward the Ph.D. programme. The authors also acknowledge the DST–FIST programme at V.O. Chidambaram College, Thoothukudi, for providing the necessary infrastructure and instrumental facilities.

Author contributions
Annmaria K. George- Writing—original draft, Methodology, Funding acquisition, M. Suresh Gandhi-review & editing, Visualization, Supervision, Project administration, P. Muthukumar- Writing—review & editing, Conceptualization, Data curation, Resources, Priyadarsi D. Roy- Writing—review & editing, Investigation, Project administration, A. Baalamurugan- Data curation, Resources, Software Muralitharan Jothimani- Writing—review & editing, Data curation, Resources, Visualization, S. Selvam- Writing—original draft, writing—review & editing, Investigation, Project administration.

Funding
No funding is available for this study.

Declarations

Competing interests
The authors declare no competing interests.

Ethics approval
The study did not require ethical approval since it did not involve human subjects and/or animals.

Consent for publication
All the authors have given consent for submission and subsequent publication of the manuscript.

Consent to participate
All the authors agreed for authorship, and read and approved the manuscript.

Additional information
Correspondence and requests for materials should be addressed to M.J. or S.S.

Reprints and permissions information is available at www.nature.com/reprints.

Publisher's note Springer Nature remains neutral with regard to jurisdictional claims in published maps and institutional affiliations.

Open Access This article is licensed under a Creative Commons Attribution-NonCommercial-NoDerivatives 4.0 International License, which permits any non-commercial use, sharing, distribution and reproduction in any medium or format, as long as you give appropriate credit to the original author(s) and the source, provide a link to the Creative Commons licence, and indicate if you modified the licensed material. You do not have permission under this licence to share adapted material derived from this article or parts of it. The images or other third party material in this article are included in the article's Creative Commons licence, unless indicated otherwise in a credit line to the material. If material is not included in the article's Creative Commons licence and your intended use is not permitted by statutory regulation or exceeds the permitted use, you will need to obtain permission directly from the copyright holder. To view a copy of this licence, visit http://creativecommons.org/licenses/by-nc-nd/4.0/.

© The Author(s) 2026